INTERFEROMETRIC OBSERVATIONS OF THE OPTICAL DISPERSION OF AMMONIA IN THE NEAR INFRARED

ARTHUR C. O'LEARY
AND
WILLIAM R. LAUTERBACH

INTERFEROMETRIC OBSERVATIONS OF THE OPTICAL DISPERSION OF AMMONIA IN THE NEAR INFRARED

* * * * *

Arthur C. O'Leary, Jr.

William R. Lauterbach

INTERFEROMETRIC OBSERVATIONS OF THE OPTICAL DISPERSION OF AMMONIA IN THE NEAR INFRARED

by

Arthur C. O'Leary, Jr.
Commander, United States Navy

and

William R. Lauterbach
Captain, United States Air Force

Submitted in partial fulfillment of
the requirements for the degree of

MASTER OF SCIENCE
IN
PHYSICS

United States Naval Postgraduate School
Monterey, California

1 9 5 8

INTERFEROMETRIC OBSERVATIONS OF THE OPTICAL DISPERSION OF AMMONIA IN THE NEAR INFRARED

by

Arthur C. O'Leary, Jr.

and

William R. Lauterbach

This work is accepted as fulfilling
the thesis requirements for the degree of
MASTER OF SCIENCE
IN
PHYSICS

from the
United States Naval Postgraduate School

ABSTRACT

This investigation was undertaken at the U. S. Naval Postgraduate School, Monterey, California, between 20 January 1958, and May 1958, by Commander Arthur C. O'Leary, Jr., USN, and Captain William R. Lauterbach, USAF.

The optical dispersion of ammonia in the infrared has previously been determined by measuring the refraction of a monochromatic beam by a gas filled prism, but the method has some troublesome systematic errors in a spectral region where the absorption bands are as numerous as in the near infrared spectrum of ammonia. Believing that interferometric techniques would be free of systematic errors and would yield more precise results than the prism method in the near infrared, we used a Rayleigh type interferometer to measure the spectrum in that region as far as the available equipment would permit. The value of such dispersion measurements lies in the fact that, while they give the same information about molecular structure as absolute intensity measurements, they give more accurate data in the areas where it is possible to make them.

We wish to express our appreciation to Professor Sydney H. Kalmbach for his suggestion of this project as well as for his assistance in pursuing it, and to Mr. M. K. Andrews and Chief Opticalman A. N. Goodall, USN, for their assistance and advice during the construction and setting up of our equipment.

TABLE OF CONTENTS

LIST OF ILLUSTRATIONS

TABLE OF SYMBOLS

L	Length of optical path in medium under investigation
ΔP	Pressure differential between chambers of the refraction tube
T	Temperature in ^{o}K
a	Slit width
b	Distance between double slits
d	Center to center distance of double slits
f	Focal length
k	Absorption Coefficient
m	Fringe Count
n	Index of refraction
s	Distance between macima in fringe pattern
ν	Fundamental vibration band
λ	Wave length
ω	Frequency
ω_o	Resonant Frequency

CHAPTER I

INTRODUCTION

1. Summary

Engle and Pederson [1] constructed a relatively simple gas interferometer and with it measured the index of refraction of ammonia gas at several well defined points in the visible region of the electromagnetic spectrum. Our objective was to adapt their design to operate at the longer but invisible wave lengths of the infrared, and, if that proved feasible, to extend their investigation as far into the infrared as available equipment would allow. The greatest obstacle appeared to be the location of a detector with the ability to resolve the intensity variations of the necessarily weak diffraction pattern.

A detailed discussion of our apparatus may be found in Chapter II. Suffice it to say that we used an uncooled lead sulfide cell whose published range is from about 1.1μ to about 3.0μ. Within this range for ammonia, Herzberg [2] reports ten overtone and combination bands, three identified as "strong" and three others as "medium". Unfortunately, we were only able to get readable response from 1.3μ to 2.5μ although this is readily understandable when one considers that the maximum of both the source intensity and detector sensitivity curves occurs at about 2.0μ and that we were constantly operating at the maximum gain of our amplifier. Even this response was only possible with the strictest attention to optical alignment, something which proved to be extremely critical, almost perversely variable, and very easily disturbed by such things as

vibrations in the building or variations in the ambient temperature. A description of our procedures and techniques will be found in Chapter III and our results are in Chapter IV.

2. The Ammonia Molecule

The ammonia molecule is a "symmetric top" [2] in the shape of a triangular pyramid with the nitrogen atom at the apex and the three hydrogen atoms at the vertices of the base, as shown in Figure 1. It is a polar molecule with the negative charge of the nitrogen atom balanced by the center of the three hydrogen atoms. There are six possible vibration bands for a

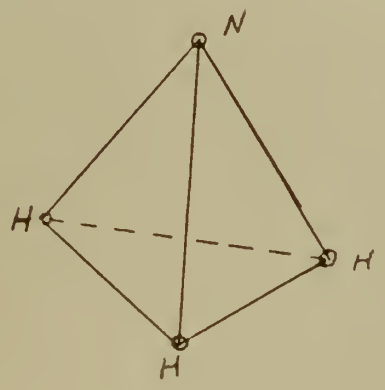

Figure 1. Structure of the Ammonia Molecule

four atomic molecule, but, in this case two doubly degenerate ones appear, leaving us a total of four which are discrete. All are well known, and all are above the wave length region we covered, but, as previously mentioned, there are many overtone and combination bands between 1 and 2.5μ, making this a fruitful field for investigation

3. Index of Refraction Determination

The absolute index of refraction of a gas is defined to be

the ratio of the velocity of an electromagnetic wave in a vacuum to the velocity of the same wave in the gas; and is, of course, a function of wave length. Though indices may be measured in any of several ways; interferometric techniques have proven to be quite accurate and convenient.

Essentially, in this procedure, one starts with a monochromatic point source, or as close to a point as is practical. He then collimates the beam, provides for part of it to travel in one medium and part in another, then permits the parts to recombine. Due to the difference in optical path taken by the two portions of the original beam, they can be made to form so called "interference fringes" upon recombination. If one then is able to admit a known density of the gas in question into one of the paths without changing the other, the effective optical path is changed, and the fringe pattern will shift its position.

If the change is slow enough and continuous, it will appear that the fringes are steadily moving toward the medium of higher index of refraction. Now if one counts the fringes which appear to pass a given point, we may find the difference in the refraction indices by the following formula:

$$n_2 - n_1 = \frac{m\lambda}{L}$$

where n_2 is the index in the gas and n_1 is that of the standard. Correcting to standard temperature and pressure (0°C and 760 mm Hg), as well as using a vacuum for the standard medium, changes this to:

$$n-1 = \frac{m\lambda}{L} \cdot \frac{T}{27318} \cdot \frac{760}{\Delta P}$$

Slater and Frank [3] show the relation between the index of refraction and the absorption coefficient, both considered as functions of frequency. As frequency increases, the index of refraction exhibits the phenomenon of anomalous dispersion at each of the resonant frequencies while the absorption coefficient remains small everywhere except for a peak at each of the resonant frequencies. The relation between index of refraction and absorption coefficient is shown in Figure 2.

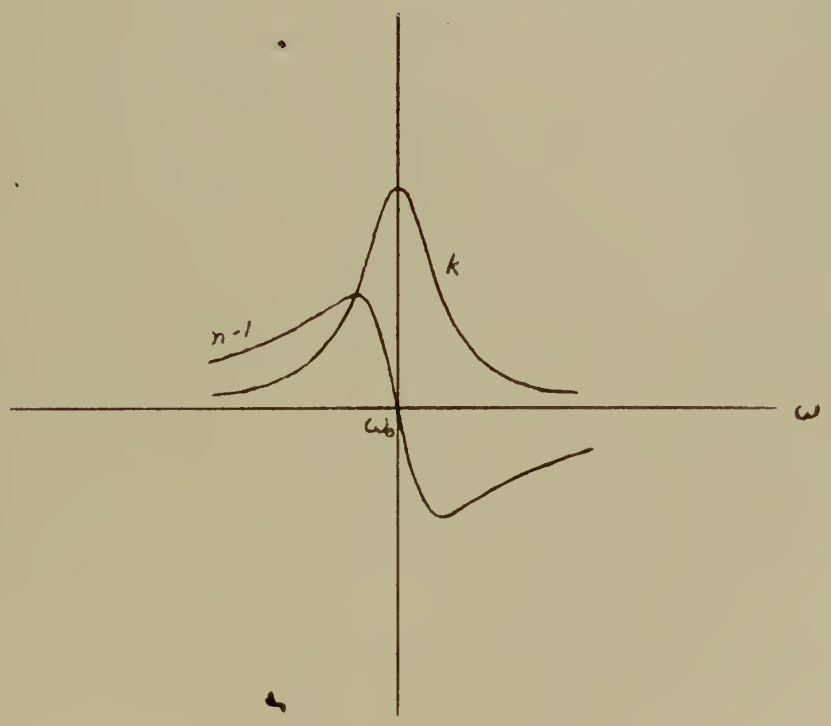

Figure 2. Index of Refraction and Absorption Coefficient as Functions of Frequency

CHAPTER II

APPARATUS

1. General

The major component parts of the experimental equipment are illustrated in Figures 3 through 5 and consist of the following:

a. A Perkin - Elmer Infrared Spectrophotometer, Model 13, which was used as a generating source for that portion of the infrared spectrum under consideration as well as a monochromator for wave length selectivity.

b. A Rayleigh Interferometer permitting insertion of the subject gas into the optical path of the selected energy and the formation of interference fringes.

c. A detector system for the purpose of counting the fringe shifts during the period of gas admission.

d. An electronic amplifier and recorder system for processing the detector signals and displaying them on a strip chart.

e. A vacuum system for clearing the refractometer tube of impurities and reducing the pressure therein to one one-hundredth of a millimeter of mercury.

f. A mercury manometer for measuring the pressure difference between the two chambers of the refraction tube.

g. A temperature measuring device for determining the temperature of both chambers of the refraction tube during an experimental run.

h. A gas distillation and admission system for purifying the sample gas and maintaining control of its entrance into the gas section of the refractometer tube.

2. Perkin-Elmer Infrared Spectrophotometer

The purpose of the Perkin-Elmer Spectrophotometer was to deliver a monochromatic beam of infrared energy to the Rayleigh interferometer entrance slit. It is fully described in [4] , and Figure 3 schematically illustrates those portions which were utilized. In order to secure maximum output energy from the Nernst glower, which was manually controlled at an operating current averaging. 9 amperes, the single beam mode of operation was used. The radiation chopper, producing a 13 cycle per second signal at the detector for the purpose of eliminating external signals, was set at the lead sulfide detector synchronous position. In the monochromator, a NaCl prism was installed and the scatter plate removed from the normal optical path so that infrared energy could pass out of the instrument. Also the slit micrometer was set to read zero when the entrance slit, S_1, had just closed while the exit slit, S_2, remained slightly open.

3. Rayleigh Interferometer

The exit slit of the monochromater served as the source slit for the Rayleigh interferometer. Its pattern was picked up by a plane mirror which reflected the beam to a 14 degree off axis parabolic mirror which served as a collimator. The parallel beam from the collimating mirror was delivered to the refraction tube by means of a second plane mirror in such a manner that rays of approximately equal intensity traversed each channel.

The refraction tube used is that described by Engle and

Pederson [1] with the substitition of KBr for glass windows and the insertion of springs around the securing bolts of the cover plates in order to prevent damage to the windows at high pressures. Mounted on the exit end of the tube was a double slit mask cut from the manila folder. The dimensions of this mask are listed in the appendix in conjunction with the computations for the detector slit width. Schematically, the interferometer is represented in Figure 4.

4. Detector System

A twin of the collimating parabolic mirror was positioned at the end of the refractometer tube in order to intercept the double slit pattern and focus it on the detector slit. A slit assembly from a Gaertner monochromator was mounted on the detector assembly housing in such a position that the 7.92 inch focus requirement of the ellipsoid focusing mirror would be satisfied as well as to permit ease in setting the proper slit width demanded by the particular wave length being used. A slit setting, $a = 19\lambda$, isolated one half of a fringe from the double slit pattern and permitted its passage to the ellipsoid mirror for focusing and delivery to the lead sulfide detector. In this manner, intensity maxima and minima would be exposed to the detector effectively establishing a pattern for counting each fringe's passage.

5. Electronic Amplifier and Recording System

In the amplifier, the electrical output signal of the detector was filtered, rectified and discriminated in favor of the original 13 cps signal, was amplified, and the results were then fed to the Leeds and Northrup recorder for a strip chart presen-

tation. The travel of the pen from a minimum through a maximum and back to a minimum represented the shift of one fringe past the detector slit.

6. Vacuum System

Since the limit of accuracy of the manometer measurements was one-tenth of a millimeter, the vacuum system was so designed and constructed that a vacuum of approximately .01 mm of mercury could be obtained, and a rise of less than .1 mm held throughout the duration of an experimental run. For measuring purposes, a calibrated Pirani gauge and bridge was attached to the system. A liquid air cooled trap was installed ahead of the vacuum fore pump for the purpose of freezing impurities that may have entered the system and isolating previously used ammonia samples. The system is illustrated in Figure 5.

7. Mercury Manometer

Pyrex glass tubing was carefully joined in order to arrive at a length which would permit the travel of mercury representing a pressure change of two atmospheres. Approximately five pounds of distilled mercury was introduced into the manometer and two cathetometers placed in such positions that mercury levels in both sides of the manometer could be read simultaneously. This was made necessary due to changes in the diameter of the pyrex glass tubing introduced while joining and also served to correct for small diameter fluctuations throughout its length. A calibration curve was drawn up for the manometer for a region of mercury travel greater than those incurred during any experimental determination.

8. Temperature Device

A copper-constantan thermocouple connected to a Rubicon bridge assembly provided temperature measurements of both chambers of the refractometer tube to the accuracy of one quarter of one degree centigrade.

9. Gas Distillation and Admission System

Two liquid air pyrex glass traps mounted in tandem and separated by three way stopcocks from each other and the vacuum system permitted fractional distillation of the commercial ammonia gas for the purpose of purification prior to its use in the refractometer tube. The delivery trap was conveniently mounted so that very delicate control of the entry of the gas could be maintained by raising and lowering its allied liquid air dewar vessel.

CHAPTER III

PROCEDURES

1. System Checks and Optical Alignment

While the fore pump was evacuating the complete system to approximately .01 mm of mercury, sufficient anhydrous ammonia for several runs was introduced into the gas admission system. The minimum guaranteed purity of the gas was quoted to be 99.5% by the Matheson Co., Inc., Newark, California; but furthur purification was carried out in order to remove the .5% impurities. This was accomplished by fractional distillation between the two traps using liquid air. At least three distillation cycles were carried out before the final product was frozen in the admission control trap to await bleeding into the gas chamber of the refraction tube.

A rate of rise versus time check on the vacuum system was then made with the vacuum pump turned off in order to determine whether or not the system would remain below .1 mm of mercury for the period of time necessary to make an experimental run.

While this process was being accomplished, the alignment of the optical system was made. Light from a mercury arc was focused on the entrance slit of the monochromator with the wave length set for the strong green line at the exit slit. By adjusting the collimating mirror and the two plane mirrors of the Rayleigh Interferometer, beams of parallel light of approximately equal intensity were caused to traverse each chamber of the refraction tube.

A small removable mirror was positioned in the detector housing barrel behind the detector slit and a microscope mounted above it with a focus on the slit so that the double slit pattern could be observed. Adjusting the parabolic mirror at the end of the refractometer tube brought the fringe pattern into sharp focus for proper alignment on the slit jaws. These procedures permitted visual checking of the clarity and regularity of the double slit pattern in order to insure that a half fringe section could be isolated and would be presented to the detector.

Finally, the light from the detector slit was focused on the detector by adjusting the ellipsoidal mirror. It must be remarked that the optical alignment was extremely critical and easily disrupted. The first indication that alignment was not true was a non-varying detector signal or none at all.

After the wave length drum had been positioned at the setting corresponding to the wave length of the intended run, the slit width, $a = 19\lambda$, was set on the detector slit. With the Perkin - Elmer Spectrophotometer in full operation, the presentation of a detector signal on the strip chart was verified. Optimum presentation was obtained by positioning the console controls and setting the micrometer slit. On the average, 50 microns was the smallest setting which would give a readable fringe pattern.

2. Experimental Run Techniques

Having brought the entire vacuum system down to a proper operating region, the fore pump was removed from the system and turned off. The vacuum and gas chambers of the refraction

tube were isolated from each other and the initial readings on both cathetometers recorded. Removal of the liquid air dewar from the admission control trap started bleeding of the sample gas into the gas chamber of the refraction tube and its rate of entry was finely controlled by strategic positioning of the dewar below the trap itself. This fine control was necessary for interpretation and ease of reading of the fringe pattern on the recording chart.

When an average of about 75 fringes had been recorded, simultaneous readings were taken on both cathetometers, the position of the pen at the time of reading marked and a temperature of both sides of the refraction tube measured. Throughout the run, care was taken to see that the pressure on the vacuum side of the refraction tube remained below .1 mm mercury as measured on the Pirani gauge; if it reached this value, the run was terminated. Normally the experimental run would be considered completed when the fringe count became uncertain because of reduced intensity or the total gas pressure had reached approximately one atmosphere.

Replacement of the liquid air dewar on the admission control trap removed the sample gas from the tube and recovered it for subsequent runs. The gas chamber was connected to the vacuum system and the fore pump engaged in order to sweep the system of any residue gas and reduce the pressure to the starting point of the next run.

3. Expected Accuracy

An estimate of the maximum error in the value of the observed index of refraction can be made by considering the indi-

vidual effects of error in measurement in all of the quantities used to calculate the refractive index. Differentiation of the formula:

$$n = 1 + \left(\frac{760}{273.18}\right)\left(\frac{m \lambda T}{L \Delta P}\right)$$

leads to:

$$\frac{dn}{n} = \frac{dm}{m} + \frac{d\lambda}{\lambda} + \frac{dT}{T} - \frac{dL}{L} - \frac{d(\Delta P)}{\Delta P}$$

An error in the measurement of the length of the refraction tube would effect all observed values of the index of refraction in the same direction and amount; hence it is treated as a constant. Its magnitude was estimated to be:

$$\frac{dL}{L} = \frac{1.05|}{74.6} = .067\ \%$$

Inserting design limitation values of the instruments, estimated personnel errors, and using average values of m, T, and P, we arrive at the following values for individual measurement errors.

$$\frac{dm}{m} = \frac{1.25|}{74.3} = .337\ \%$$

$$\frac{dT}{T} = \frac{1.25|}{295} = .085\ \%$$

$$\frac{d(\Delta P)}{\Delta P} = \frac{1.35|}{416} = .084\ \%$$

Hence the maximum expected error in the refractive index due to measured variables on any one run is estimated to be:

$$\frac{dn}{n} = .337 + .085 + .084 \cong .5\ \%$$

This error should be reduced in the final result by taking a mean of several runs. Since $d\lambda$ is involved in any particular series of runs, the error in refractive index would be increased by this factor. From our calibration curve of wave length versus drum setting, we estimate our error in wave length could be:

$$\frac{d\lambda}{\lambda} = \frac{1\,1\,1}{230} = .435\,\%$$

Summing these values then, the total error in the observed refraction index can be as great as 1%.

CHAPTER IV

RESULTS

Our equipment as assembled, and when precisely aligned optically for a sharp double slit diffraction pattern at the detector slit, proved capable of reproducibly distinguishing between maxima and minima through most of the detector sensitivity range. (The sensitivity curve for the lead sulfide cell used is shown in Figure 7.) However the signal to noise ratio is small, a fact principally due to the vibrations set up by an unbalanced chopper assembly. This noise was particularly offensive, of course, because it tended to occur at the same 13 cycle per second frequency as the desired signal.

The solution to the noise difficulties was to keep the period of the signal quite long, the ideal being about one fringe passage in two minutes. Figure 8 is an acutal trace cut from the center of a recorded run and is close to the ideal. Usually, though, control this accurate was extremely difficult to obtain and even more difficult to maintain, so a variable but much longer period was normally accepted. Unfortunately, this increased the time necessary for an average run to something on the order of five hours, obviously putting very stringent limitations on the number of points we could investigate in the time available.

Eleven points selected at random were studied, as well as one purposely selected in the center of an absorption region given by [2] . The results are plotted in Figure 9, in company with all bands given by [2] , and a curve denoting the

index of refraction extrapolated from the data for the visible region as given in [5] . Tables 1 and 2 show our results in comparison with those extrapolated from both sets of data for the visible region from [5] . All values in Table 1 have been adjusted to 0°C and 760 mm Hg. All those in Table 2 have been adjusted to a number of molecules per unit volume equal to Avogadro's number divided by 22.414 liters.

Table 1. Refractive Indices of Ammonia at 0°C and 760 mm Hg.

	$(n-1)\times10^8$		
$\lambda(\mu)$	O'Leary and Lauterbach	Cuthbertson and Cuthbertson	Lovia and Patkowski
*1.315	39749	37250	37408
1.466	38968	37203	37357
*1.622	36740	37169	37319
1.670	37568	37160	37310
1.748	37835	37147	37295
1.918	37690	37124	37271
*2.135	35098	37102	37247
2.175	36780	37099	37243
2.193	36948	37098	37242
*2.238	34337	37094	37238
*2.368	35056	37086	37229
2.477	36788	37080	37222

*Considered as anomalous values because of known or suspected absorption bands nearby.

Table 2. Refractive Indices of Ammonia at 2.687×10^{22} molecules per liter

$\lambda(\mu)$	$(n-1)\times10^8$ O'Leary and Lauterbach	Cuthbertson and Cuthbertson	Lovia and Patkowski
*1.315	39151	36690	36845
1.466	38382	36644	36795
*1.622	36188	36610	36758
1.670	37003	36601	36749
1.748	37266	36588	36734
1.918	37123	36566	36711
*2.135	34570	36544	36687
2.175	36227	36541	36683
2.193	36392	36540	36682
*2.238	33821	36536	36678
*2.368	34529	36528	36669
2.477	36248	36522	36662

*Considered as anomalous values because of known or suspected absorption bands nearby.

CHAPTER V

CONCLUSION

1. Evaluation of Data

Our data has been plotted in Figure 9 without a curve and only in order to present a qualitative picture of the general trend of the index of refraction of ammonia in the near infrared. Also plotted, for comparison purposes, is the same index extrapolated from visible spectrum data of [5]. The precise significance of our data is indeterminate in view of the paucity of points that it was possible to cover. However, one may rightfully question the ability of any smooth curve to depict anything more than a general trend in an area where almost random variations occur as often as is the case here.

Three significant features do appear, however. First, the experimental indices of refraction nearest the visible wave lengths are very considerably greater than the values obtained by extrapolating the visible curve into the infrared. Second, when tests were made at or near wave lengths reported in [2] to be absorbed, the indices observed had greater variations from surrounding than would normally be expected. Third, additional anomalies, suggesting additional absorption bands, were found at two points well removed from bands previously reported.

It may be that these two additional anomalies are due to combination and/or overtone bands not reported in [2]. Using the values of the fundamentals given by McKean and Schatz [6], we find as a possibility that there is a $5\nu_2$ band near 2.135μ and a ν_1 plus $3\nu_2$ and/or a $2\nu_4$ plus $3\nu_2$ band near 1.622μ.

2. Future Possibilities

The apparatus as presently set up can, of course, be used to completely and precisely map the infrared spectrum of ammonia in the region we have only been able to survey. With a stronger source and/or a cooled detector, it should even be possible to extend the region somewhat on either side. However, advancement to much longer wave lengths would obviously require a different detector, and we know of none with sufficient sensitivity in those areas.

The present equipment can also be used for interferometric study of other gases in which the near infrared is of interest. HCl appears to be an excellent subject along this line, and it would be considerably easier to analyze because of its simpler structure and the resulting reduction of the number of combination bands.

Of the possible physical improvements, the most promising is the use of a Cassegrainian mirror between the exit slit of the monochromator and the refraction tube. This would serve the triple purpose of shortening the air path of the energetic beam, reducing the complexity of the optical path, and replacing three individually mounted mirrors with two integrally mounted ones.

Finally, a different refraction tube seems highly desirable. The present one has served admirably for a feasibility study, but, as may be seen in the Appendix, our permissible detector slit width is a function of the wave length, the focal length of the decollimating mirror, and the reciprocal of the distance between centers of the double slits. The wave length

is a natural constant, and an increase in the focal lenght of the decollimator appears undesirable because it would also increase the already great difficulty in aligning the system optically. The third factor, separation of the double slits, is controlled by the thickness of the wall between chambers of the refraction tube. Our tube is the product of joining two single chambers, both of copper, and consequently has an abnormally thick center wall. Making the tube of stronger material and fabricating it as a unit would be a sizeable improvement.

BIBLIOGRAPHY

1. R. K. Engle and D. M. Pederson, Design and Construction of Instrumentation for Investigating the Optical Dispersion of Ammonia Gas, U. S. Naval Postgraduate School, Monterey, Calif., 1956.

2. G. Herzberg, Infrared and Raman Spectra of Polyatomic Molecules, D. Van Nostrand Co., Inc., New York, 1945.

3. J. C. Slater and N. H. Frank, Electromagnetism, McGraw-Hill Book Co., Inc., New York, 1947.

4. Model 13 Ratio Recording Infrared Spectrophotometer Operating and Maintainence Instructions, The Perkin-Elmer Corp., Norwalk, Conn., 1955.

5. International Critical Tables, Vol. VII, McGraw-Hill Co., Inc., New York, 1930.

6. D. C. McKean and P. N. Schatz, Absolute Infrared Intensities of Vibration Bands in Ammonia and Phosphine, J. Chem. Phys., 24-2, pp 316-325, February 1956.

7. W. E. Williams, Applications of Interferometry, John Wiley & Sons, Inc., New York, 1950.

APPENDIX I

DETERMINATION DETECTOR SLIT SETTING

Williams [7] gives the formula for the angle between interference maxima of a Rayleigh interferometer as,

$$\theta = \frac{\lambda}{a+b} \qquad \text{or} \qquad \theta = \frac{\lambda}{d}$$

Geometrically, the angle is that whose sine is the linear distance between successive maxima at the detector slit divided by the focal length of the decollimating mirror,

$$\sin \theta = \frac{S}{f}$$

This is further equal to the angle itself in the case of angles as small as this, so $\frac{S}{f} = \frac{\lambda}{d}$

Measurements showed $a_1 = 3.458$ mm

$a_2 = 3.155$ mm

$b = 3.872$ mm

$f = 267$ mm

Therefore,

$$d = \frac{a_1 + a_2}{2} + b = 7.18 \text{ mm}$$

and $$\frac{S}{f} = \frac{\lambda}{7.18} \qquad \text{or} \qquad S = \frac{267}{7.18}\lambda$$

In order to read alternating maxima and minima at the detector, the slit width should be about s/2 or about 19 λ.

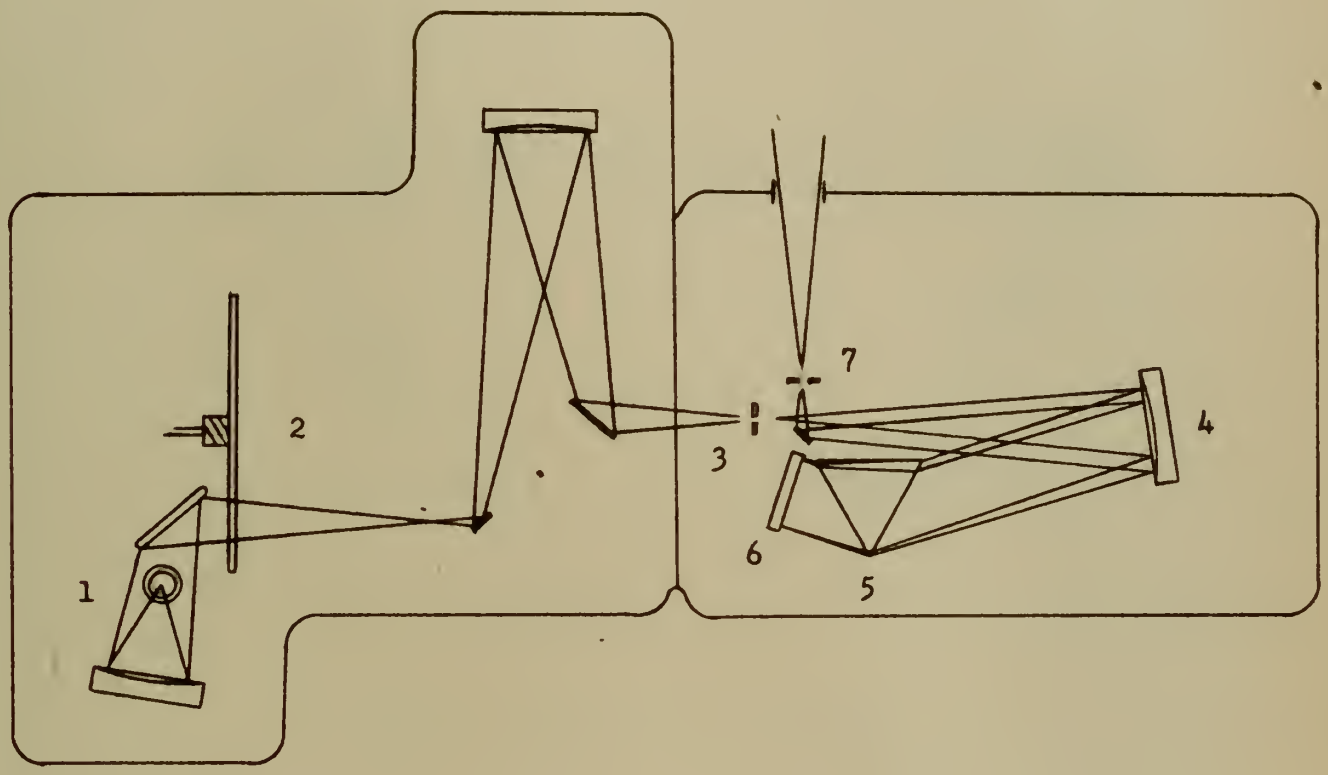

Figure 3. Source and Monochromator

Legend

1. Source - Nernst Glower
2. Chopper
3. Entrance Slit
4. Collimator Mirror
5. NaCl Prism
6. Littrow Mirror
7. Exit Slit

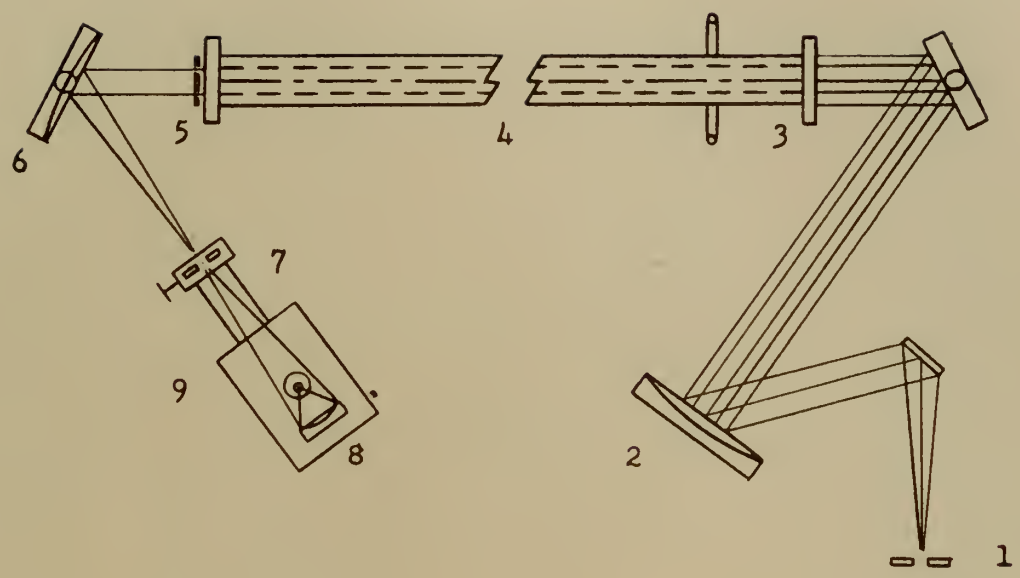

Figure 4. Rayleigh Interferometer

Legend

1. Exit Slit of Monochromator
2. Collimator Mirror
3. KBr Window
4. Refractometer Tube
5. Double Slit
6. Focusing Mirror
7. Detector Slit
8. Ellipsoid Mirror
9. PbS Detector

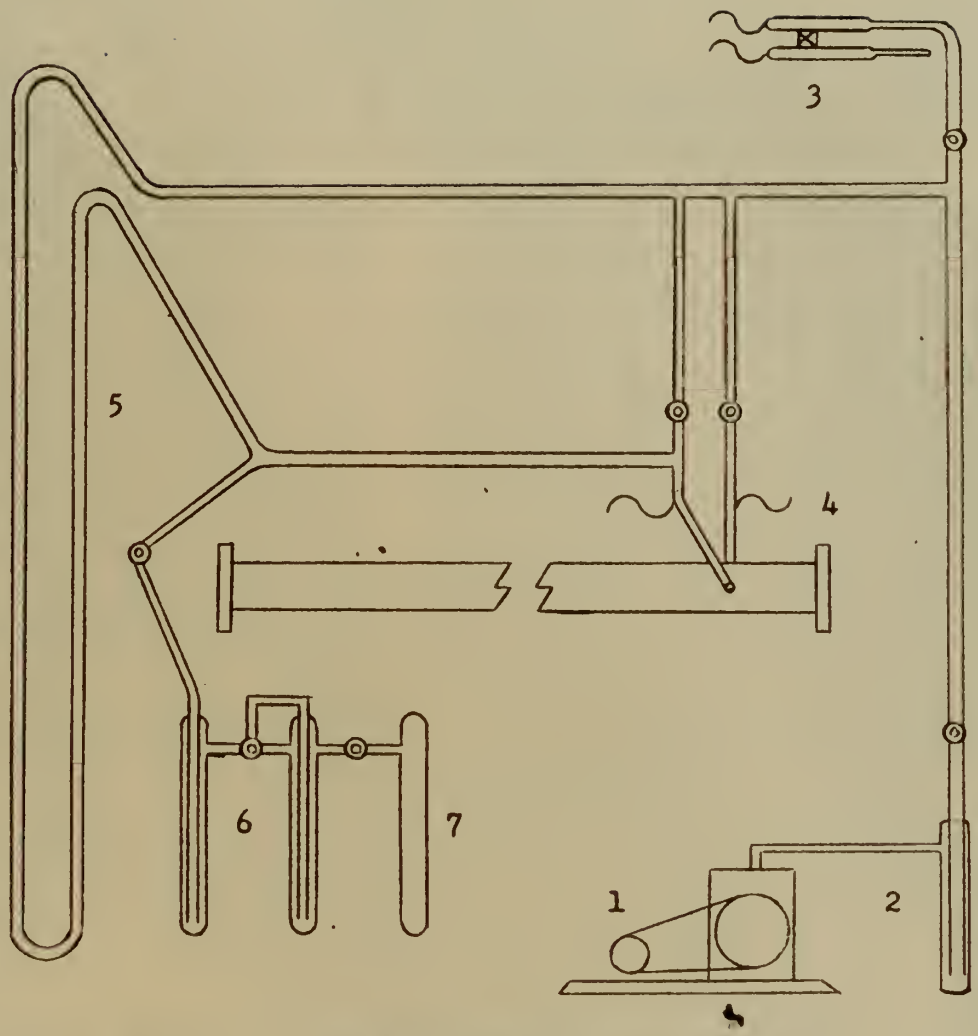

Figure 5. Vacuum and Distillation Systems

Legend

1. Vacuum Fore Pump
2. Residue Trap
3. Pirani Guage
4. Thermocouple
5. Manometer
6. Distillation Traps
7. Ammonia Supply

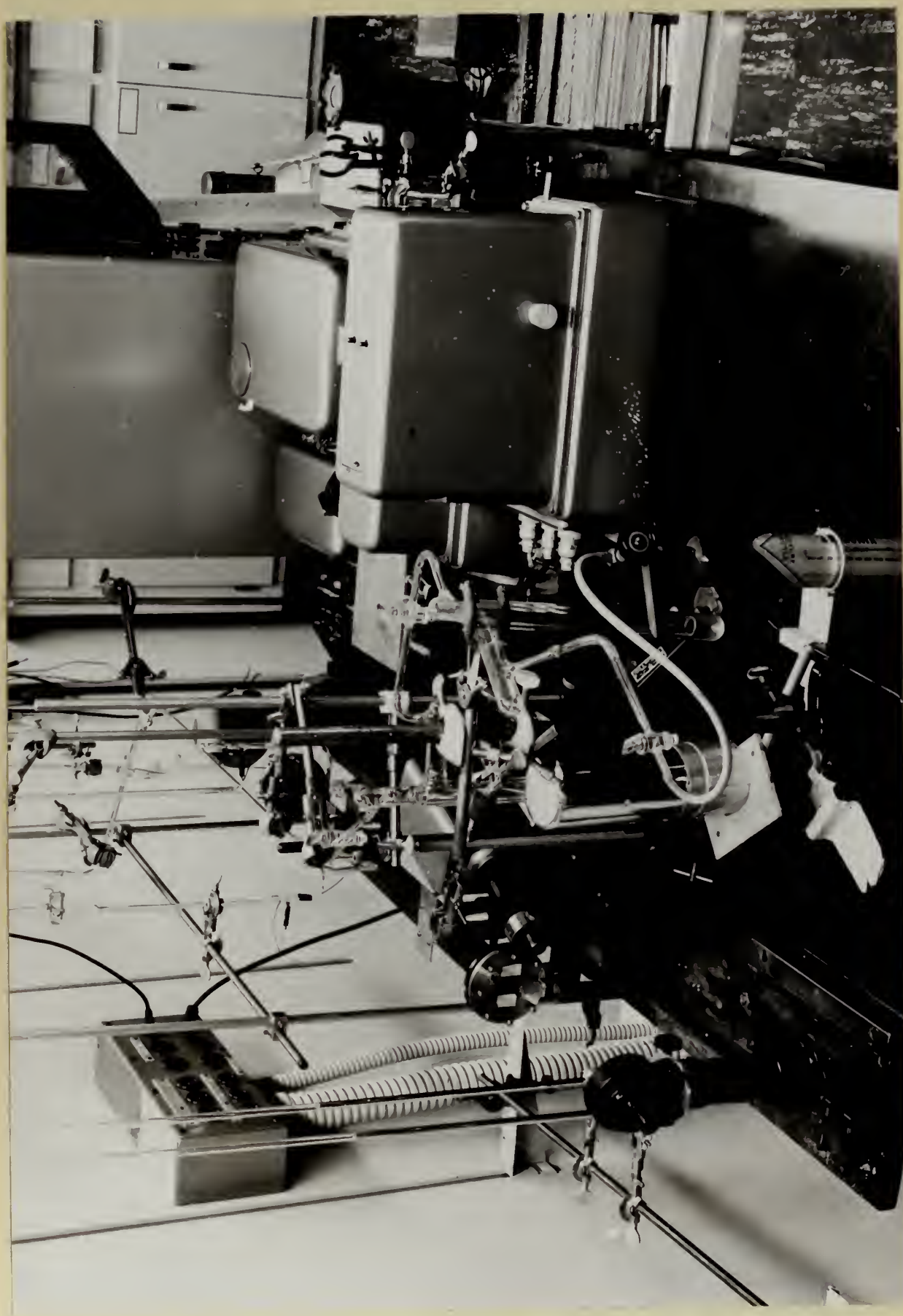

Figure 6. Composite Arrangement of Equipment

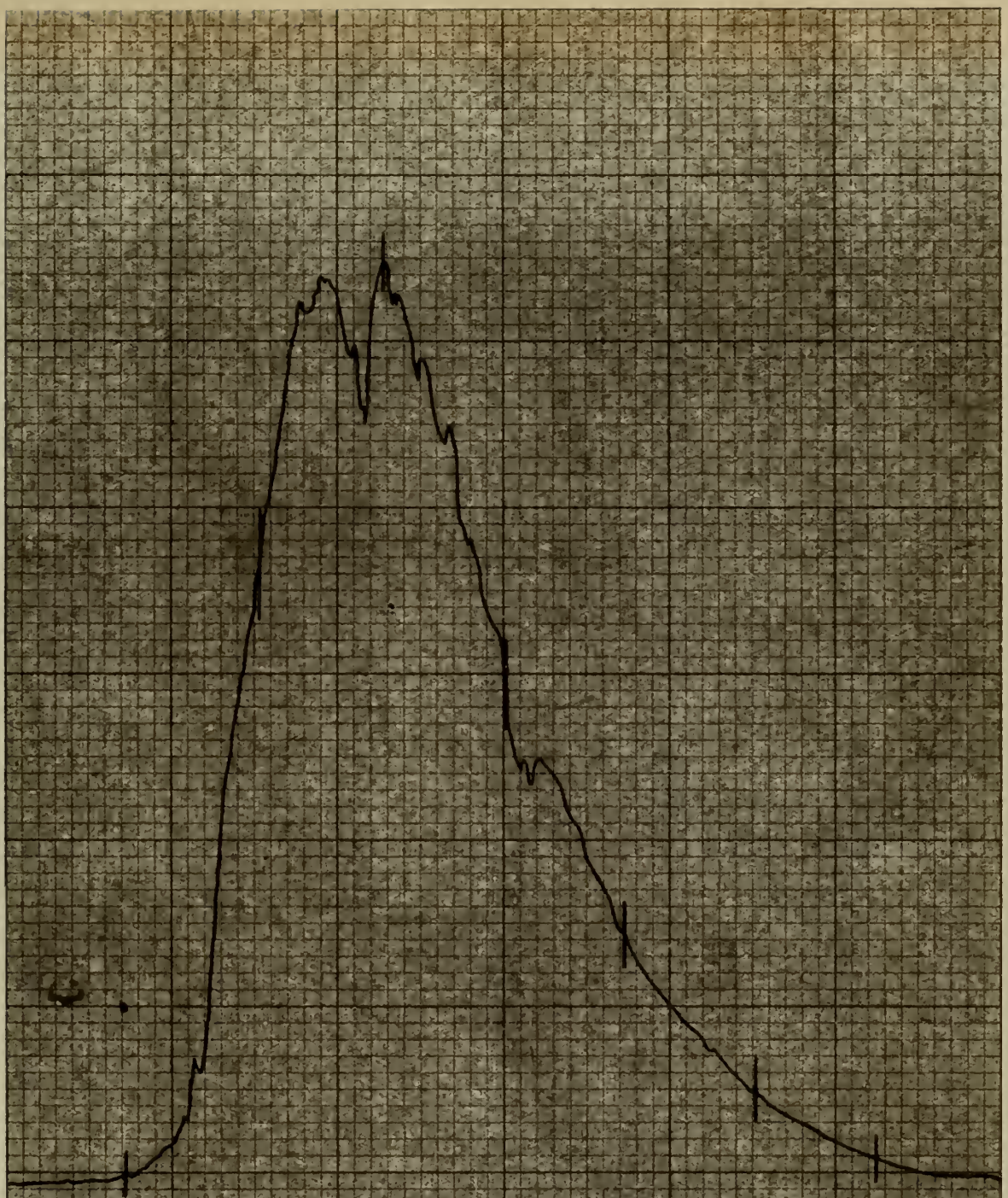

Figure 7. Sensitivity Curve for Lead Sulfide Detector

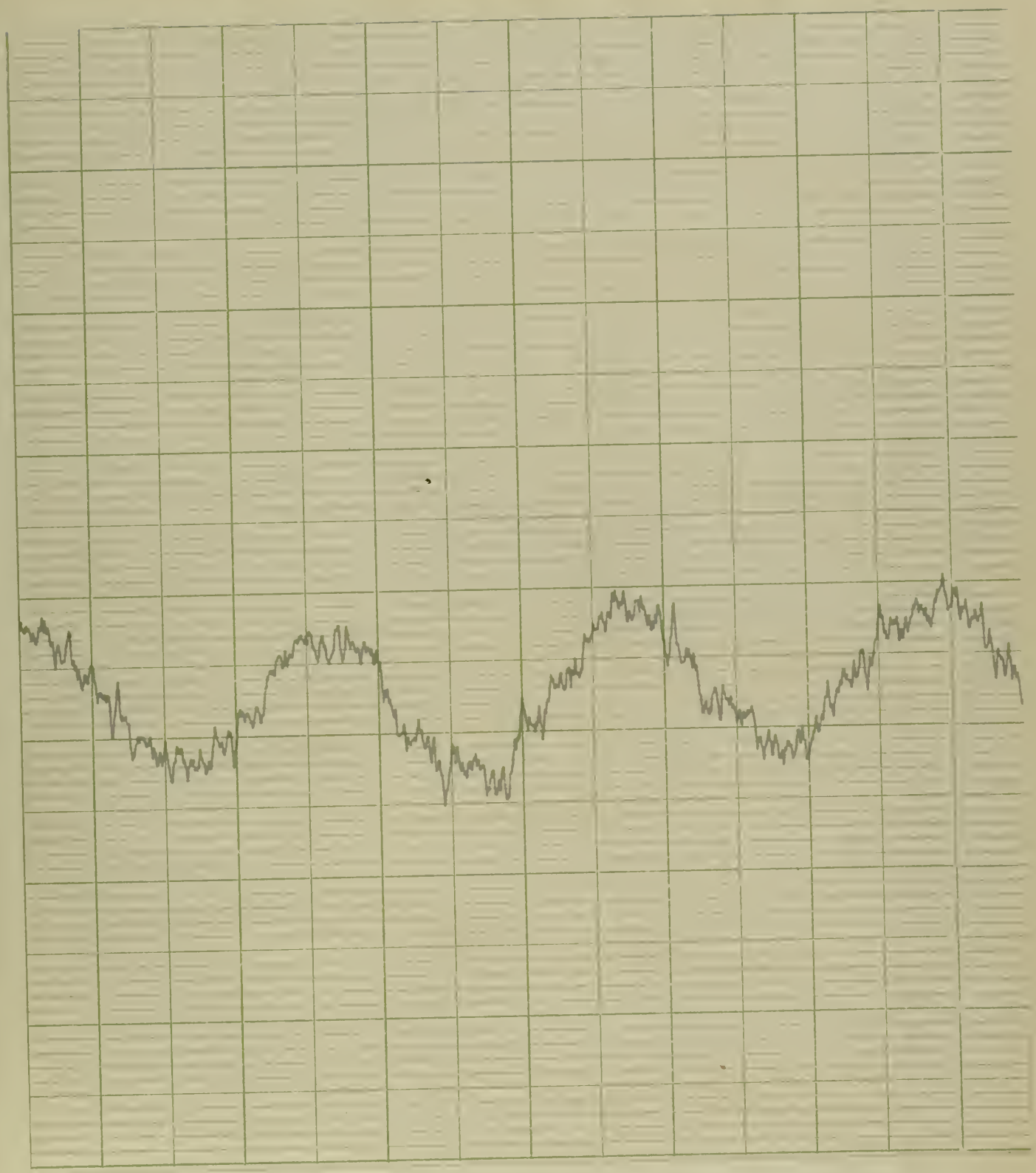

Figure 8. Fringe Pattern as Recorded